Research Article

Fluorescent Silica Nanoparticles in the Detection and Control of the Growth of Pathogen

Kethirabalan Chitra and Gurusamy Annadurai

Environmental Nanotechnology Division, Sri Paramakalyani Centre for Environmental Sciences,
Manonmaniam Sundaranar University, Alwarkurichi, Tamil Nadu 627412, India

Correspondence should be addressed to Gurusamy Annadurai; gannadurai@hotmail.com

In this present study the bioconjugated fluorescent silica nanoparticles give an efficient fluorescent-based immunoassay for the detection of pathogen. The synthesized silica nanoparticles were polydispersed and the size of the silica nanoparticles was in the range of 114–164 nm. The energy dispersive X-ray spectrophotometer showed the presence of silica at 1.8 kev and the selected area diffractometer showed amorphous nature of silica nanoparticles. The FTIR spectrum confirmed the attachment of dye and carboxyl group onto the silica nanoparticles surface. The fluorescent silica nanoparticles showed highly efficient fluorescence and the fluorescent emission of silica nanoparticles occurred at 536 nm. The SEM image showed the aggregation of nanoparticles and bacteria. The growth of the pathogenic *E. coli* was controlled using silica nanoparticles; therefore silica nanoparticles could be used in food packaging material, biomedical material, and so forth. This work provides a rapid, simple, and accurate method for the detection of pathogen using fluorescent-based immunoassay.

1. Introduction

The fundamental building blocks of nanotechnology are nanoparticles [1]. The particulate dispersions or solid particles with a size in the range of 10–1000 nm are called nanoparticles [2]. Silica is encompassed of a honeycomb-like porous structure with hundreds of empty channels. Due to their unique properties such as high surface areas, large pore volumes, tuneable pore sizes with a narrow distribution, and tuneable particle diameters, currently silica nanoparticles have been intensively investigated in materials research [3]. Because of their simple preparation and possible applications in several fields, dispersed, uniform, and amorphous silica nanoparticles have produced specific interest [4].

Generally two methods are being used for the preparation of silica nanoparticles, such as microemulsion which is used to prepare the dye-doped and magnetic nanoparticles and stober method which is used to prepare pure silica and organic dye doped silica nanoparticles. The morphology of the nanoparticles can be controlled through the parameters involved in the process [5]. In stober process, due to the hydrolysis process, the ethoxy groups are replaced by TEOS; the hydrolysis reaction initiates by the attachment of hydroxyl anions on TEOS molecules [6, 7]. The condensation reaction occurs immediately after hydrolysis reaction. The Si–O–Si bridges are formed by the alcohol condensation of hydroxyl group of intermediate reaction with ethoxy group of other TEOS, or the water condensation of hydroxyl group of another intermediate by hydrolysis reaction [7, 8].

In biotechnological and information technologies applications, the fluorescent nanoparticles are excellent as an indicators and photon sources. Currently, in biology and medicine, fluorescent silica nanoparticles have appeared as an attractive fluorescent probe and engrossed extensive attention. Various biomedically important targets, such as cancer cells, bacteria, and individual biomolecules could be labelled with highly fluorescent silica NPs that have emerged in biomedical field [9, 10]. A two-step process is involved in the synthesis of fluorescent silica nanoparticles: the first one is the dye chemically bound to an amine-containing silane agent, followed by APTES and TEOS that are hydrolysed together to form dye-doped silica nanoparticles [11].

The silica has entrenched surface chemistry which allows for the surface functionalization of silica nanoparticles with

various functional groups such as amino, carboxyl, thiol, and methacrylate [12]. Various techniques include layer-by-layer assembly, physical adsorption, and silane coupling agents (co hydrolysis), are commonly used for the functionalization of silica nanoparticles surface. Among these techniques, silane functionalization method is widely used for the silica surface modification. The covalent bond formation occurs between the surface silanol groups and silane coupling agents during the silane functionalization process [13, 14]. The cohydrolysis process is carried out by mixing suitable amount of organosilane with TEOS which facilitates particles conjugation and particle dispersion; various functional groups such as thiol, amine, carboxyl groups, and phosphonate groups could be attached by using this method [15, 16]. In this present work, silica nanoparticles surface is modified with carboxyl group with the help of silane coupling agent EDC. The carboxyl group modification process provides the well-dispersed nanoparticles and reduces the aggregation of silica nanoparticles and these water soluble surface functionalized nanoparticles can further be conjugated with biomolecules for biological applications [12, 17].

In this work, the surface modified fluorescent silica nanoparticles were prepared and used for control of the growth and detection of pathogen. The synthesized silica nanoparticles were spherical in shape and they polydispersed in size. The fluorescent silica nanoparticles excitation was found at 480 nm and emission occurred at 526 nm. Silica nanoparticles showed well antibacterial activity against *E. coli*.

2. Experiments

2.1. Materials. Triethoxy orthosilicate, 3-aminopropyltriethoxysilane (APTES) nitric acid, ethanol, 1-ethyl-3-(3-dimethylaminopropyl)-carbodiimide (EDC), phosphate buffer, 2-(N-morpholino) ethanesulfonic acid buffer (MES) and N-hydroxysuccinimide (NHS), ethanol, and ammonia were purchased from Himedia India Pvt. Ltd., Mumbai. *E. coli* culture was obtained from Microlabs, Institute of Research and Technology, Arcot. Antibody (*E. coli* (1011) sc-57709) was purchased from Santa Cruz Biotechnology, INC Europe.

2.2. Preparation of Surface Modified Fluorescent Silica Nanoparticles. In a clean vessel 1.57 mL of ammonia (solvent), 37 mL of ethanol (solvent), and 5 mL of water was added together. The mixture was stirred for 5 min then 3 mL of TEOS was added to the mixture and stirred for 1 hr. The silica nanoparticle was recovered by centrifugation at 10,000 rpm for 30 min. The pellet was dried in hot air oven at 60°C.

1 mM of the amine reactive dye was mixed with 1.5 mL of dimethylformamide. The solution was stirred for 1 hr followed by 1 M of 3-(aminopropyltriethoxy silane) that was added to the mixture and stirred for 24 hr and then 1 g of dried silica nanoparticles was added to the aqueous solution. The reaction was carried out for 24 hrs, followed by centrifugation at 10,000 rpm for 30 min to collect fluorescent silica nanoparticles. The particles were dried at 60°C for 4 hr.

The carboxyl group modified fluorescent silica nanoparticles were prepared as follows. In a clean 50 mL beaker 10 mg of fluorescent silica nanoparticles was mixed in 1 mL

of 0.1 M phosphate buffer (pH 7.4) and 20 μL of 1-ethyl-3-(3-dimethyl aminopropyl)-carbodiimide. The mixture was stirred for 4 hrs, and after 4 hrs of reaction the nanoparticles were centrifuged at 10,000 rpm for 30 min and washed with ethanol and distilled water several times. Then the particles were air-dried at 60°C for 4 hrs. The carboxyl surface modified fluorescent nanoparticles were characterized and used to detect the pathogenic bacteria.

2.3. Characterization of the Synthesized Nanoparticles. The nature of the prepared silica nanoparticles was observed using powder X-ray diffractometer (X'per PRO model) and CuKα radiation at 40 keV in the range of 20–80. Further, the morphology of the prepared nanoparticles was characterized by using scanning electron microscopy (HITACHI Model S-3000H). Energy dispersive X-ray diffractometer (Thermo SuperDry II) was used to analyse the element of the nanoparticles. The size of the synthesized silica nanoparticles was examined using transmission electron microscopy (JEOL-2010) and the selected area diffractometer was used to analyes the crystalline nature of the nanoparticles. The Fourier transform infrared spectroscopy analysis (MAKE, BRUKER Optik GmbH, Model no. TENSOR 27, OPUS version 6.5 software) was performed to know the possible functional groups of silica nanoparticles. The UV-spectrofluorometer was used to determine the fluorescence excitation and emission spectra of silica nanoparticles and the fluorescence microscope was used to analyse the fluorescence ability and also used to detect the pathogen.

2.4. Pairing of Antibody with Nanoparticles. The suspension of surface modified NPs was centrifuged at 10,000 rpm for 10 min and washed with distilled water and the pellet was dispersed in 1 mL of 0.1 M MES buffer, followed by 0.5 mL aqueous solution of 10 mM sulfo-NHS and 4 mM of EDC dissolved in MES buffer was added immediately to the nanoparticles solutions and the NPs suspension was incubated at room temperature with agitation. After 15 min of incubation the NPs were centrifuged at 10,000 rpm for 10 min and washed with 0.1 M of phosphate buffer (pH 7.4); then the nanoparticles were resuspended in 1.5 mL of phosphate buffer and then 100 μL of monoclonal antibody at the concentration of 0.1 mg/mL was added to the nanoparticles solution. After 2 hrs of reaction the conjugated nanoparticles were centrifuged and washed with phosphate buffer (0.1 M) several times and resuspended in phosphate buffer.

2.5. Control of the Growth of Pathogen Using Surface Modified Silica Nanoparticles. The different concentration of silica nanoparticles was used for determination of antibacterial activity of silica nanoparticles. The various concentrations of silica nanoparticles (20 μL, 50 μL, and 100 μL) were added into the LB medium and then *E. coli* culture was inoculation into the medium followed by incubated at room temperature in orbital shaker. The optical density of the broth was taken at 620 nm for different time intervals.
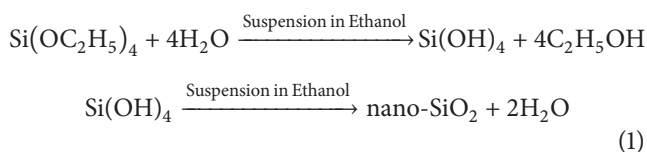
2.6. Bacteria Conjugated with Antibody Conjugated Nanoparticles. *E. coli* was grown at room temperature in nutrient

broth for 16 hr on orbital shaker. 100 μL of 0.1 mg/mL of antibody conjugated silica nanoparticles added with 500 μL of 16 hrs bacterial sample. Then the suspension was incubated for 10–15 min, followed by the suspension was centrifuged at 10,000 rpm for 15 min to remove the unbound antibody conjugated nanoparticles with bacteria and washed with phosphate buffer for several times. Then the pellet was used for the detection of pathogen.

3. Results and Discussion

In highly supersaturated solution, a huge number of primary particles are first nucleated, and then the stable particles are formed by the rapid aggregation of primary particles. As a result, the monodispersed spherical-shaped particles were formed in the suspension [7].

The chemical reaction of the silica nanoparticles preparation and the hydrolysis and polycondensation reactions are as follows:

$$Si(OC_2H_5)_4 + 4H_2O \xrightarrow{\text{Suspension in Ethanol}} Si(OH)_4 + 4C_2H_5OH$$

$$Si(OH)_4 \xrightarrow{\text{Suspension in Ethanol}} \text{nano-}SiO_2 + 2H_2O$$

(1)

3.1. Morphological Characteristics of Silica Nanoparticles.
Figure 1 shows the XRD pattern of stober silica NPs. The XRD spectrum of the silica nanoparticles shows that the synthesized silica nanoparticles are amorphous in nature. The XRD spectrum indicates a characteristic broad halo peak at 20° revealing the amorphous nature of the silica particles. The broad peak of XRD pattern stated, a high percentage of the silica particles are amorphous [18]. The 2θ value of the present XRD spectrum result was compared and confirmed by using standard JCPDS file and the obtained XRD result is matched with JCPDS file (79-1711); hence, XRD results confirmed that the synthesized material is amorphous silica particles.

Figure 2 shows the SEM and EDX images of the synthesized silica nanoparticles via stober method. Figure 2(a) shows that the synthesized silica nanoparticles are in spherical shape and the size of NPs is in the range of 151 nm to 165 nm, and also the unevenly distributed agglomerated spherical particles are present. Similarly, Venkatathri obtained polydispersed spherical silica particles with the size in the range of 100–200 nm [19].

Figure 2(b) shows the EDX spectrum of the synthesized silica nanoparticles. In the EDX results confirm the occurrence of strong signal features of elemental silica. Silica nanoparticles display an optical absorption band peak at approximately 1.8 keV and also the EDX reveals the presence of the impurities such as oxygen and carbon elements. Sajid and Devasena have reported that a strong Si peak occurred at 1.8 keV and also they noticed O and C element in EDX spectrum [20].

Figure 3 shows the TEM image of the synthesized silica nanoparticles. Figure 3(a) shows the various sizes of the silica nanoparticles synthesized via a stober method. The TEM images illustrate the spherical, polydispersed silica nanoparticles. The size of the synthesized silica nanoparticles
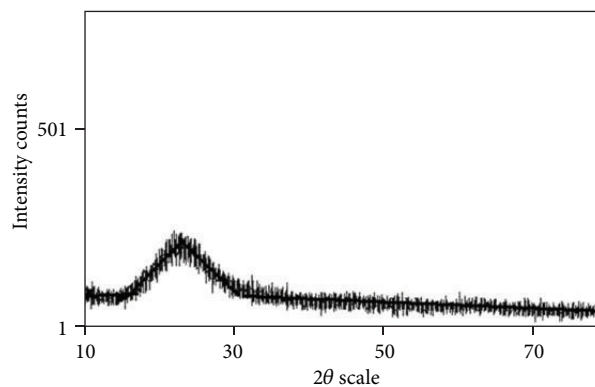

Figure 1: XRD spectrum of silica nanoparticles.

is in the range of 114 nm–168 nm. Similarly, Chandran et al. reported without aggregated polydispersed particles and the size in the range of 200 nm [14]. An earlier study reported that during the nucleation process, any parameter which increases the rate of the hydrolysis process has a tendency to produce fewer nuclei; thus larger particles are formed at last [7]. Figure 3(b) shows the SAED pattern of the synthesized silica nanoparticles; the amorphous nature of the silica nanoparticles is confirmed using SAED pattern; there is no well-defined diffraction ring of synthesized silica nanoparticles. Yang et al. reported the similar result for SAED pattern they obtained SAED pattern without any defined ring [21].

Figure 4 shows the FTIR spectrum of silica, fluorescent silica, and carboxyl group modified silica nanoparticles. Figure 4(a) shows the FTIR spectrum of silica nanoparticles; the bands at 468 cm^{-1}, 799 cm^{-1} and 1093 cm^{-1} are the main characteristic peaks of Si–O–Si bonds vibrational modes, which are recognizes to O–Si–O vibrational band, Si–O bending vibrational band, and Si–O–Si stretching vibration band, respectively [22–24]. The band at 1629 cm^{-1} reveals the presence of O–H bending vibration of adsorbed molecular water and the peak at 2926 cm^{-1} indicates the presence of unreacted TEOS in the silica particles. The absorbance band at 3420 cm^{-1} indicates the hydrogen bonded Si–OH stretching vibration of silica nanoparticles [25].

Figure 4(b) shows the fluorescent silica nanoparticles FTIR spectrum; the bands at 2895 cm^{-1} and 2831 cm^{-1} represent the stretching vibrations of C–H bonds, and they show that a few organic groups are attached on the surface of silica NPs [19]. The band at 1022 indicates Si–O–Si vibrational stretching and the bands at 3615 cm^{-1} and 3170 cm^{-1} indicate the bond interaction between the organic dye and silica particles [26]. The band at 1562 cm^{-1} designates the N–H bending vibrations of primary amine group.

Figure 4(c) shows the FTIR spectrum of carboxyl group modified silica nanoparticles. The band at 3433 cm^{-1} indicates the carboxyl group attached at the surface of synthesized silica particles. The peak at 1635 cm^{-1} donates the hydroxyl group [20]. The peaks at 1055 cm^{-1}, 799 cm^{-1}, and 460 cm^{-1} indicate the Si–O–Si bonds stretching vibration modes.

3.2. Fluorescence Studies.
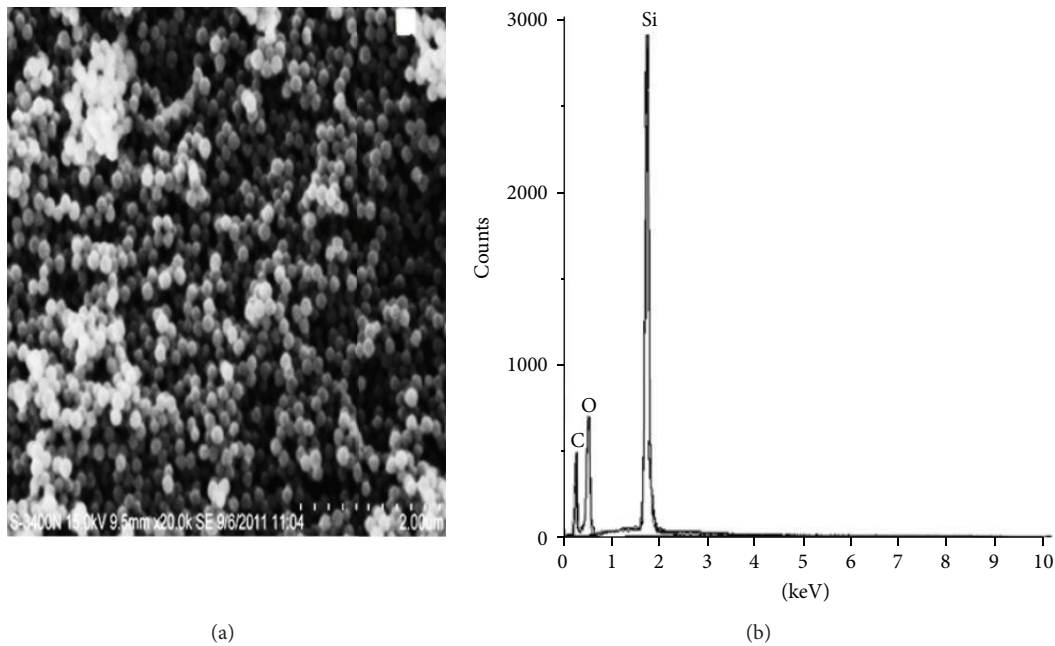Figure 5(a) shows the excitation and emission spectra of silica. The excitation and emission

(a)

(b)

Figure 2: (a) Scanning electron microscopy image and (b) EDAX image of stober silica nanoparticles.
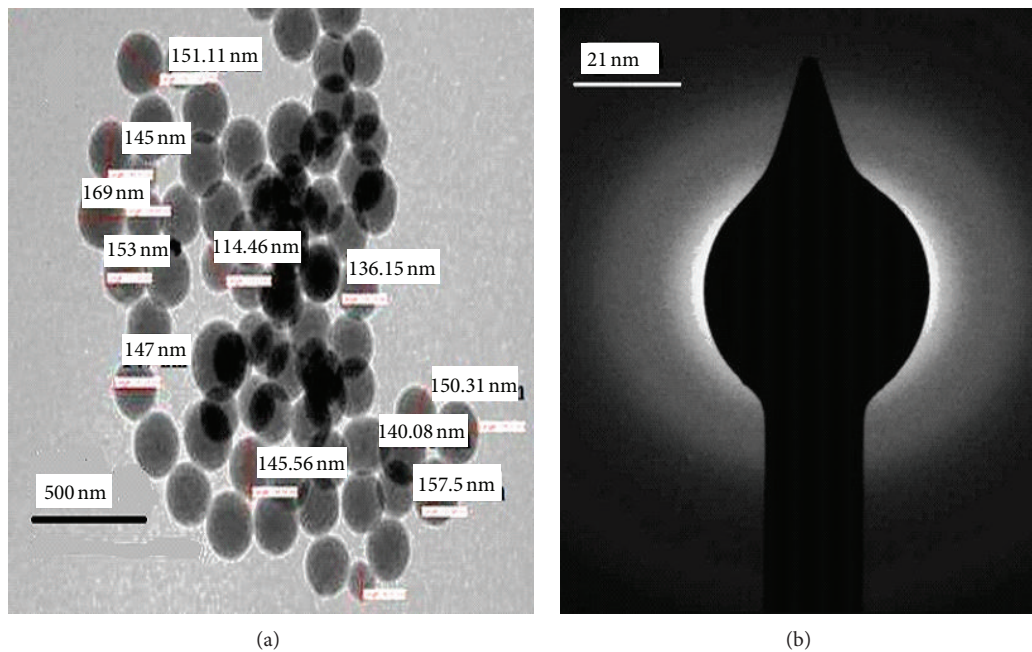

(a)

(b)

Figure 3: (a) TEM image and (b) SAED pattern of surface modified fluorescent silica nanoparticles.

of dye-doped silica NPs occur at 480 nm and 535 nm. Santra et al. reported that the emission and excitation of spectra remain the same for the pure Rubpy and LDS nanoparticles. They proved that there is no change in the emission intensity for the LDS nanoparticles and also they stated that the luminophores were well protected inside the silica network in normal atmosphere [27]. Figure 5(b) shows the fluorescence image of silica nanoparticles. Canton et al. reported that the highly luminescent dye doped silica nanoparticles synthesized via modified stober method and they have reported

the fluorescent nanoparticles can be used for the bioanalysis and bioanalytical experiments [28].

3.3. Application of Silica Nanoparticles. The growth rate of biomass was compared with and without addition of silica nanoparticles with biomass. Figure 6 shows the antibacterial effect of silica NPs. The maximum growth inhibition of *E. coli* occurred at 100 μL of silica nanoparticles.

Song et al. reported similar results; they have stated the bacterial adhesion inhibition by the quaternary ammonium
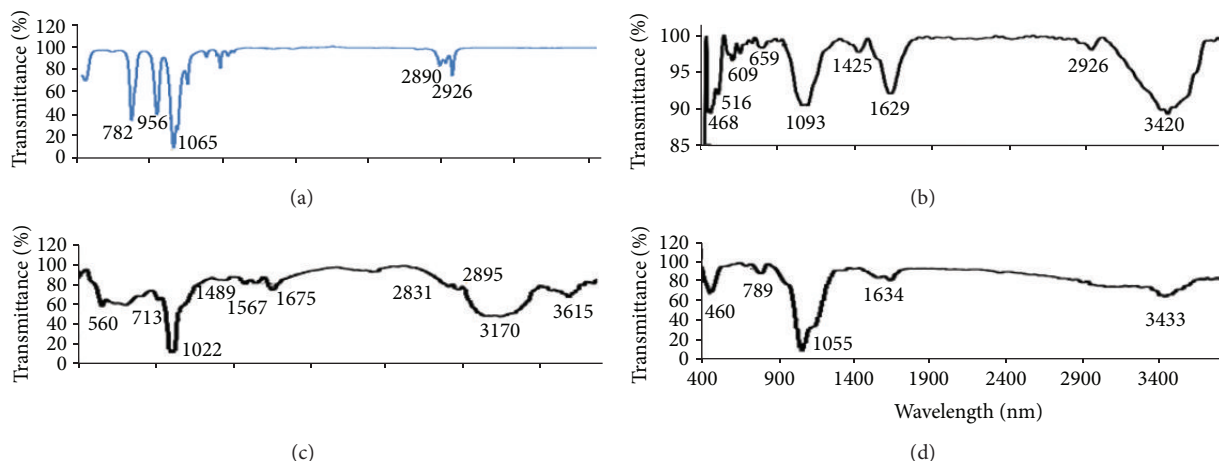
Figure 4: FTIR Spectrum of (a) TEOS, (b) silica, (c) fluorescent silica and (d) surface modified silica nanoparticles.
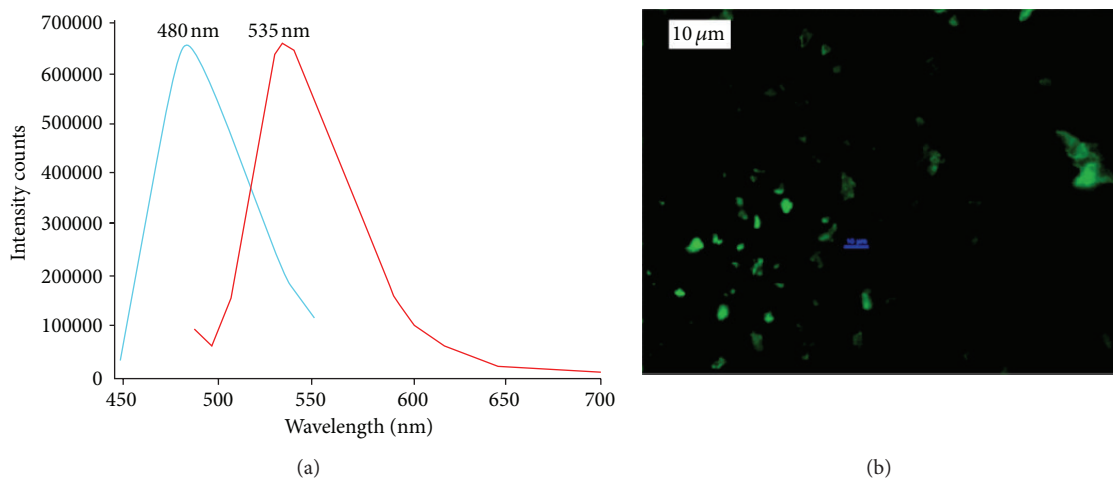

Figure 5: (a) Excitation and emission spectra and (b) fluorescence image of silica nanoparticles.
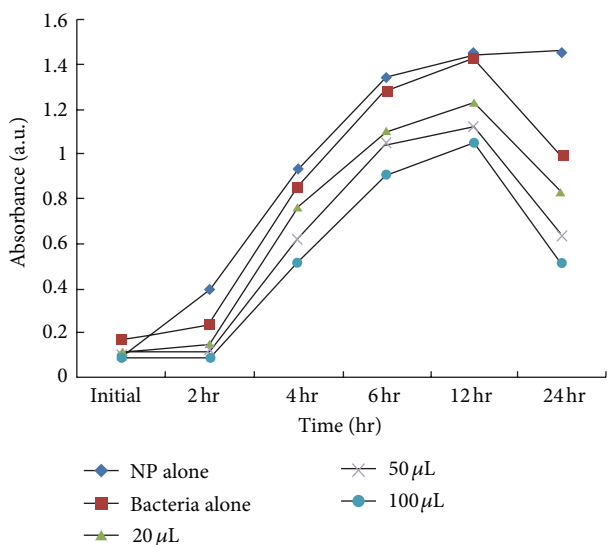

Figure 6: Antibacterial activity of silica nanoparticles against *E. coli*.

functionalized silica NPs. They proved that the bacteria were seriously damaged in their outer membrane and lost their cellular reliability of bacterial species while contacting with silica-QAS core shell NPs. Thus, the positively charged QAS-modified silica NPs interacted with the lipid bilayer structures of the bacterial membranes, which led to the death of cells. Due to the water-repelling properties and the positive charge of the QAS-modified silica NPs, adhered bacteria were directly eradicated. The antibacterial activity of NPs was influenced by the size of the NPs [29].

Figure 7 shows the fluorescent image of *E. coli* at ×60 magnification. Figure 7(a) shows that many fluorescent NPs were coupled with the bacterial cell; thus, the NPs provide highly proficient fluorescence-based immunoassay. The SEM image shows the aggregation of bacteria and nanoparticles; thus, it illustrates that so many antibodies conjugated silica NPs are bind with bacterial cell. The SEM image was taken at 6 Kv accelerating voltage and worked at ×57 magnification (Figure 7(b)). The amine holding antibody was conjugated onto the carboxyl functional group found on the surface of

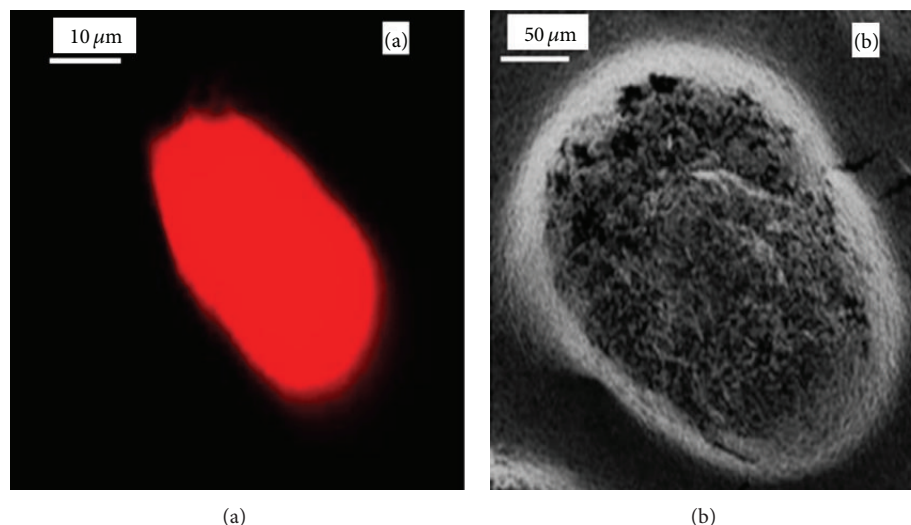(a)   (b)

FIGURE 7: (a) Fluorescence image of bacteria and (b) SEM image of bacteria after being incubated with antibody conjugated silica nanoparticles.

NPs. Each single fluorescent silica NP has tens of thousands of fluorescent dye; thus, the dye-doped silica NPs have the capability to show high intensification [30]. Due to the lack of heavy metal silica NPs are nontoxic. Silica NPs are greater material for microscopic imaging of cells in vivo because of their noncytotoxic properties along with their innate dispersivity [31]. Because of their higher density, silica NPs can be easily centrifuged during preparation, functionalization, and other solution treatment processes and the fluorescent silica NPs showed high photostability and provided easy surface modification process and they are inert so protect the dye from external factors [32]. Thus, a single bacterial cell was detected rapidly and exactly using silica nanoparticles. Similarly Zhao et al. detected the pathogen within 20 min by using antibody conjugated fluorescent silica NPs [33].

4. Conclusion

The surface modified fluorescent silica nanoparticles were prepared using a simple, nontoxic method. In this present study, amorphous, spherical-shaped silica nanoparticles were synthesized. The silica nanoparticles showed good antibacterial activity against pathogenic *E. coli*; thus, silica nanoparticles could be used as an antibacterial agent in many fields. The silica nanoparticles were used as fluorescent-based nanoprobe for detection of pathogen.

Conflict of Interests

The authors declare that they have no conflict of interests.

Acknowledgments

References

[1] A. Leela and M. Vivekanandan, "Tapping the unexploited plant resources for the synthesis of silver nanoparticles," *African Journal of Biotechnology*, vol. 7, no. 17, pp. 3162–3165, 2008.

[2] V. J. Mohanraj and Y. Chen, "Nanoparticles—a review," *Tropic Journal of Pharmaceutical Research*, vol. 5, no. 1, pp. 561–573, 2006.

[3] H. Wanyika, E. Gatebe, P. Kioni, Z. Tang, and Y. Gao, "Synthesis and characterization of ordered mesoporous silica nanoparticles with tunable physical properties by varying molar composition of reagents," *African Journal of Pharmacy and Pharmacology*, vol. 5, no. 21, pp. 2402–2410, 2011.

[4] L. P. Singh, S. K. Bhattacharyya, G. Mishra, and S. Ahalawat, "Functional role of cationic surfactant to control the nano size of silica powder," *Applied Nanoscience*, vol. 1, no. 3, pp. 117–122, 2011.

[5] W. Tan, K. Wang, X. He et al., "Bionanotechnology based on silica nanoparticles," *Medicinal Research Reviews*, vol. 24, no. 5, pp. 621–638, 2004.

[6] C. J. Brinker and G. W. Scherer, *Sol-Gel Science: The Physics and Chemistry of Sol-Gel Processing*, Academic Press, San Diego, Calif, USA, 1990.

[7] I. A. M. Ibrahim, A. A. F. Zikry, and M. A. Sharaf, "Preparation of spherical silica nanoparticles: stober silica," *The Journal of American Science*, vol. 11, pp. 985–989, 2010.

[8] K.-S. Kim, J.-K. Kim, and W.-S. Kim, "Influence of reaction conditions on sol-precipitation process producing silicon oxide particles," *Ceramics International*, vol. 28, no. 2, pp. 187–194, 2002.

[9] L. Wang, K. Wang, S. Santra et al., "Watching silica nanoparticles glow in the biological world," *Analytical Chemistry*, vol. 78, no. 3, pp. 646–654, 2006.

[10] H. Ow, D. R. Larson, M. Srivastava, B. A. Baird, W. W. Webb, and U. Wiesnert, "Bright and stable core-shell fluorescent silica nanoparticles," *Nano Letters*, vol. 5, no. 1, pp. 113–117, 2005.

[11] L. Wang, W. Zhao, and W. Tan, "Bioconjugated silica nanoparticles: development and applications," *Nano Research*, vol. 1, no. 2, pp. 99–115, 2008.

[12] J. E. Smith, L. Wang, and W. Tan, "Bioconjugated silica-coated nanoparticles for bioseparation and bioanalysis," *Trends in Analytical Chemistry*, vol. 25, no. 9, pp. 848–855, 2006.

[13] A. P. R. Johnston, E. S. Read, and F. Caruso, "Ultrathin, responsive polymer click capsules," *Nano Letters*, vol. 5, no. 5, pp. 953–956, 2005.

[14] S. P. Chandran, S. Hotha, and B. L. V. Prasad, "Tunable surface modification of silica nanoparticles through "click" chemistry," *Current Science*, vol. 95, no. 9, pp. 1327–1333, 2008.

[15] M. A. Markowitz, P. E. Schoen, P. Kust, and B. P. Gaber, "Surface acidity and basicity of functionalized silica particles," *Colloids and Surfaces A*, vol. 150, no. 1–3, pp. 85–94, 1999.

[16] P. Espiard, J. E. Mark, and A. Guyot, "A novel technique for preparing organophilic silica by water-in-oil microemulsions," *Polymer Bulletin*, vol. 24, no. 2, pp. 173–179, 1990.

[17] X. Wang, L.-H. Liu, O. Ramström, and M. Yan, "Engineering nanomaterial surfaces for biomedical applications," *Experimental Biology and Medicine*, vol. 234, no. 10, pp. 1128–1139, 2009.

[18] N. D. Singho and M. R. Johan, "Complex impedance spectroscopy study of silica nanoparticles via sol-gel method," *International Journal of Electrochemical Science*, vol. 7, no. 6, pp. 5604–5615, 2012.

[19] N. Venkatathri, "Preparation of silica nanoparticle through coating with octyldecyltrimethoxy silane," *Indian Journal of Chemistry A*, vol. 46, no. 12, pp. 1955–1958, 2007.

[20] P. A. R. Sajid and T. Devasena, "Synthesis and characterization of silica nanocomposites for bone applications," *International Research Journal of Pharmaceutical*, vol. 3, no. 5, pp. 173–177, 2012.

[21] T. I. Yang, R. N. C. Brown, L. C. Kempel, and P. Kofinas, "Controlled synthesis of core-shell iron-silica nanoparticles and their magneto-dielectric properties in polymer composites," *Nanotechnology*, vol. 22, no. 10, Article ID 105601, pp. 1–8, 2011.

[22] S.-R. Ryu and M. Tomozawa, "Fictive temperature measurement of amorphous SiO_2 films by IR method," *Journal of Non-Crystalline Solids*, vol. 352, no. 36-37, pp. 3929–3935, 2006.

[23] H. El Rassy and A. C. Pierre, "NMR and IR spectroscopy of silica aerogels with different hydrophobic characteristics," *Journal of Non-Crystalline Solids*, vol. 351, no. 19-20, pp. 1603–1610, 2005.

[24] L. T. Zhuravlev, "The surface chemistry of amorphous silica. Zhuravlev model," *Colloids and Surfaces A*, vol. 173, no. 1–3, pp. 1–38, 2000.

[25] A. Beganskiene, V. Sirutkattis, M. Kurtinattiene, R. Juskenas, and A. Kareiva, "FTIR, TEM, NMR investigation of stober silica nanoparticles," *Material Science*, vol. 10, no. 4, pp. 287–290, 2004.

[26] E. Albiter, S. Alfaro, and M. A. Valenzuela, "Photosensitized oxidation of 9,10-dimethylanthracene on dye-doped silica composites," *International Journal of Photoenergy*, vol. 2012, Article ID 987606, 8 pages, 2012.

[27] S. Santra, P. Zhang, K. Wang, R. Tapec, and W. Tan, "Conjugation of biomolecules with luminophore-doped silica nanoparticles for photostable biomarkers," *Analytical Chemistry*, vol. 73, no. 20, pp. 4988–4993, 2001.

[28] G. Canton, R. Ricco, F. Marinello, S. Carmignato, and F. Enrichi, "Modified Stöber synthesis of highly luminescent dye-doped silica nanoparticles," *Journal of Nanoparticle Research*, vol. 13, no. 9, pp. 4349–4356, 2011.

[29] J. Song, H. Kong, and J. Jang, "Bacterial adhesion inhibition of the quaternary ammonium functionalized silica nanoparticles," *Colloids and Surfaces B*, vol. 82, no. 2, pp. 651–656, 2011.

[30] L. Wang, C. Yang, and W. Tan, "Dual-luminophore-doped silica nanoparticles for multiplexed signaling," *Nano Letters*, vol. 5, no. 1, pp. 37–43, 2005.

[31] S. Mascharak, "Synthesis of fluorescent silica nanoparticles conjugated with RGO peptide for detection of invasive human breast cancer cells," *Nanotechnology*, vol. 3, no. 8, pp. 37–41, 2010.

[32] S. Santra, K. Wang, R. Tapec, and W. Tan, "Development of novel dye-doped silica nanoparticles for biomarker application," *Journal of Biomedical Optics*, vol. 6, no. 2, pp. 160–166, 2001.

[33] X. Zhao, L. R. Hilliard, S. J. Mechery et al., "A rapid bioassay for single bacterial cell quantitation using bioconjugated nanoparticles," *Proceedings of the National Academy of Sciences of the United States of America*, vol. 101, no. 42, pp. 15027–15032, 2004.